COMUNICACIONES DEL CIMAT

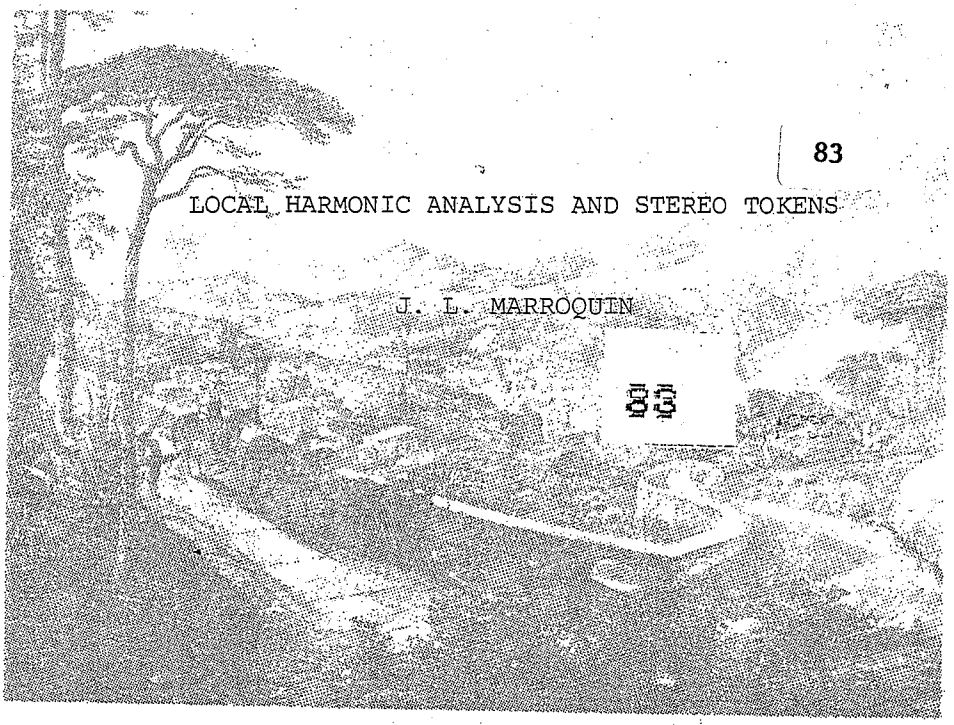

83

LOCAL HARMONIC ANALYSIS AND STEREO TOKENS

J. L. MARROQUIN

CENTRO DE INVESTIGACION EN MATEMATICAS

Apartado Postal 402
Guanajuato, Gto.
México
Tels. (473) 2-25-50
2-02-58

LOCAL HARMONIC ANALYSIS AND STEREO TOKENS

J.L. Marroquin*

*Centro de Investigacion en Matematicas

Apdo. Postal 402 ; Guanajuato, Gto. ; Mexico.

Abstract: In this paper, we discuss the problem of selecting features (tokens) that may be matched when recovering depth from stereoscopic pairs of images. A class of biologically plausible tokens, based on two-dimensional Gabor filters, is presented. It is shown that, with these tokens, one can get high quality, dense disparity maps for images of real scenes, using a very simple matching strategy. A feedback method for selecting an optimal set of filters is also presented.

0. Introduction.

In this paper we discuss the problem of recovering depth from stereoscopic pairs of images. This is an important problem in Computational Vision, and it has received a lot of attention (see, for example: Marr and Poggio, 1976; Grimson, 1981 and 1982; Baker and Binford, 1981; Mayhew and Frisby, 1981; Marroquin , 1983; Nishihara, 1984; Ohta and Kanade, 1983; Prazdny, 1985; Drumheller and Poggio, 1986). A number of effective algorithms have been developed, that perform relatively well on computer-generated "synthetic images". Their performance with images of real scenes, however, is still far below from that of biological systems.

Several issues have been recognized as fundamental for the solution of this problem:

(i) The selection of the appropriate "tokens" that should be matched along epipolar lines.

(ii) The elimination of "false targets" (the solution of the "correspondence problem").

(iii) The recovery of a dense "depth image" from the (usually sparse) disparity data.

(iv) The interacion of stereo processing with other computational modules (edge detection, texture, color, motion, etc).

In the most effective existent stereo systems, the tokens are contours, obtained from single monochromatic images (usually, as level crossings of $\nabla^2 G$ operators (see Grimson, 1982)) ; the correspondence problem is then solved by making some assumptions about the nature of the solution - specifically, that disparity varies smoothly almost everywhere. Finally, the dense disparity surface is reconstructed using some surface interpolation scheme (Grimson, 1981; Terzoupulos, 1984; Marroquin et.al. 1984, 1987; Gamble and Poggio, 1987).

In this paper, we advance the hypothesis that carefully selected tokens may simplify problems (ii) and (iii), and facilitate the solution of (iv).

1. Criteria for Token Selection.

We define a "Token" (which, informally, is a feature that is extracted from a pair of images for stereo matching) as a pair of maps :

$$T_k : I_k \subseteq \mathbb{R}^2 \quad \mathbb{R}^n \, , \; k \in \{ L,R \}$$

that assign to each point in each image I_k, a point in $\mathbb{R}^n$. In practice, a token consists in the output of n operators that act on the original images. Ideally, a token should have the following properties:

1. Density. It is preferable to have tokens that are dense (i.e., area based) rather than sparse (contour based), so that the

surface interpolation step may be eliminated.

2. Robustness. It is important that the tokens are robust with respect to the stereo transformation. This means that, if $p_l = (x_l, y_l)$ is a point in the left image, and $p_r = (x_r, y_r)$ is the corresponding point in the right one, one should have that

$$T_L(p_l) \approx T_R(p_r)$$

3. Selectivity. This means that if p_l, p_r are corresponding points , but p_l, q_r are not, one should have that

$$\| T_L(p_l) - T_R(q_r) \| > \| T_L(p_l) - T_R(p_r) \|$$

where $\| \cdot \|$ is a suitably defined norm.

4. Efficiency. As with most vision tasks, stereo matching in real time requires the use of massively parallel hardware. This means that the corresponding algorithms must be distributed, and their (parallel) complexity must be low.

5. Biological plausibility. If one is interested, not only in the design of efficient algorithms, but also in building models for biological perceptual processes, it is desirable that the building blocks of the proposed tokens are compatible with our current knowledge of neurophysiology.

6. Integration capability. It is desirable that the nature of the tokens permits the integration of other processes (color, motion, texture, etc.) into the stereo mechanism.

2. Gabor Tokens.

Our claim is that tokens that consist in the output of a selected set of two-dimensional Gabor filters ("Gabor tokens") meet the above criteria. We will now describe these filters.

A two-dimensional Gabor filter (Gabor, 1946; Daugman, 1980; Heeger, 1987) is a pair of linear, shift invariant operators, with space domain kernels given by:

$$g_c(x,y) = 1/(\sqrt{2\pi}\ \sigma)\ \exp\ [-(x^2+y^2)/2\sigma^2]\ \cos\ (2\pi ux + 2\pi vy) \qquad (1)$$

$$g_s(x,y) = 1/(\sqrt{2\pi}\ \sigma)\ \exp\ [-(x^2+y^2)/2\sigma^2]\ \sin\ (2\pi ux + 2\pi vy) \qquad (1')$$

where σ is the scale parameter, and u and v denote the x and y components of the spatial frequency (in cycles/pixel). In practice, one may truncate these kernels, for, say, $|x| > 3\sigma$ and $|y| > 3\sigma$. The power spectrum of these filters is a pair of Gaussians in the spatial frequency domain, centered at ($\pm$ u, $\pm$ v), and with standard deviation $1/2\pi\sigma$.

By varying the center frequency (u,v), one gets, for a given value of σ, a 2-parameter family of pairs of filters, whose output at a point (x,y), may be interpreted as the real and imaginary parts of the Fourier transform of the image, seen through a Gaussian window centered at (x,y), so that one may think of these filters as performing a local, 2-D Fourier analysis of an image. If I_s , I_c denote the outputs of the convolution of an image with the kernels (1) and (1'), the pair (I_s,I_c) may be called the "complex

response" of the filter, which can also be expressed as magnitude and phase using:

$$M(x,y) = \left[I_s^2(x,y) + I_c^2(x,y) \right]^{1/2}$$
$$P(x,y) = \tan^{-1}(I_s(x,y) \,/\, I_c(x,y)) \qquad (2)$$

It is interesting to note that the shape of these kernels bears a close resemblance with that of cortical cell receptive fields that have been found in mammals (Daugman, 1980), which means that tokens built with them will satisfy property (v). We will now show how to construct a system of tokens that satisfies the remaining properties.

2.1. Robustness with Respect to the Stereo Transformation.

Let us consider the formation of a stereo pair of images of a planar patch that is at a distance Z from the viewer, and with an inclination given by angles γ and β (see fig. 1).

Figure 1 around here

Suppose that this patch projects a pattern $f_l(x,y)$ in the left image (the coordinates x,y are taken with respect to the projection of the center of the patch, whose coordinates, with respect to the center of the image, are (x_l, y_l)). This pattern will be related to the corresponding one in the right image, $f_r(x,y)$ (with coordinates taken with respect to the point (x_r, y_r)

that corresponds to (x_l, y_l)) by the equation:

$$f_r(x,y) = f_l(ax + by\ ,\ y) \tag{3}$$

$$\text{where}\quad a = \cos\alpha + \sin\alpha\cot(\gamma - \alpha/2)\ ;$$

$$\cos\alpha = (Z^2 - \lambda^2) / (Z^2 + \lambda^2)\quad ;\quad \sin\alpha = 2\lambda Z / (Z^2 + \lambda^2)\ ;$$

$$\text{and}\quad b = -2\lambda\sin\beta / (\lambda\cot\gamma + Z\cos\beta)$$

In the frequency domain, if $F(u,v)$ is the Fourier transform of $f(x,y)$, we will have:

$$F_r(u,v) = \frac{1}{|a|} F_l(u/a\ ,\ v - bu/a) \tag{4}$$

From this relation, we observe that for $u = 0$, the corresponding patches in both images will have identical Fourier transforms (up to a multiplicative constant). If one is computing the local Fourier transform using Gabor filters, both sides of equation (4) have to be convolved with a gaussian that represents the transfer function of the filter. If the scale parameter σ is large, however, this gaussian will be sharp enough, so that (4) will hold approximately if we consider now F_r and F_l to be the complex responses of the corresponding filters. This means that a token that consists of a (suitably normalized) combination of Gabor filters, with center frequencies along the v axis, will satisfy

$$T_L(p_l) \approx T_R(p_r)$$

(at least for planar patches). The problem with these tokens is that we may have regions within an image where $F(u,v) \approx 0$, for

all v (i.e., patterns consisting mostly of vertical lines), which would make them extremely vulnerable to noise. For this reason, one would like to include in the tokens filters outside the v axis, provided that the errors induced by the imaging geometry are "not too large". To estimate the magnitude of these errors, we make the following considerations:

Consider a Gabor filter G_1 with center frequency (u,v), and let $F_L(u,v)$ be its output at the point p_l of the left image. From equation (4), we get that the output of the same filter, at the corresponding point p_r of the right image, will be

$$F_R(u,v) = \frac{1}{|a|} \; F_L(u',v')$$

$$\text{with} \quad \left[(u - u')^2 + (v - v')^2\right]^{1/2} = u \; \eta \; (Z \; , \; \gamma \; , \; \beta) \quad ,$$

$$\text{where} \quad \eta \; (Z \; , \; \gamma \; , \; \beta) = \left[(a - 1)^2 + b^2\right]^{1/2} / \; a \qquad (5)$$

and where a and b are defined by equation (3).

Suppose the nearest filter to G_1 is G_2, with center frequency at (w,z), and let W be the distance between (u,v) and (w,z). We will consider that the error is "acceptable", if it is less than a certain fraction h of the difference between the outputs of adjacent filters, i.e., if

$$|F_L(u',v') - F_L(u,v)| \leq h \; |F_L(u,v) - F_L(w,z)| \qquad (6)$$

Now, $|F_L(u',v') - F_L(u,v)| \leq \sup |DF_L| \left[(u-u')^2 + (v-v')^2\right]^{1/2} =$

$$= \sup |DF_L| \; u \; \eta$$

where $|DF_L|$ is the magnitude of the gradient of F_L, and the sup is taken over a neighborhood of (u,v). Assuming that W is small enough (in particular, assuming that we are sampling the frequency domain above the Nyquist rate), we may put:

$$\sup |DF_L| \approx \frac{1}{W} |F_L(u,v) - F_L(w,z)| \quad ,$$

so that $$|F_L(u',v') - F_L(u,v)| \leq \frac{u\,\eta}{W} |F_L(u,v) - F_L(w,z)|$$

so that (6) will hold if

$$\frac{u\,\eta}{W} \leq h \qquad (7)$$

To study the dependence of η on Z, γ and β, we simulated an "environment" of tilted planes in which γ and β took uniformly distributed random values in the intervals $[10^\circ, 170^\circ]$ and $[-80^\circ, 80^\circ]$, respectively, and computed the mean value of η, over 30000 samples, for several values of Z. The resulting curve is shown in fig. 2.

Figure 2 around here

From this graph one can see that in general, one can get reasonable errors, provided that the filters stay close to the v axis. Thus, for example, for a filter spacing W = 0.2, and for

h = 0.25, (7) will hold, in the average, provided that u ≤ 0.25.

In the case of the phase response, however, there is an additional factor that should be considered: the complex response of a Gabor filter with scale parameter σ and center frequency (u_o, v_o) to a pattern:

$$f(x,y) = \sin (2\pi u x + 2\pi v y + \phi)$$

$$\text{is : } {}^1/_2 \left[G (u - u_o, v - v_o)\, e^{i\phi} - G (u + u_o, v + v_o)\, e^{-i\phi}\right]$$

where G is a 2-dimensional Gaussian with scale parameter $(2\pi\sigma)^{-1}$. From this formula, one can see that the phase response will be relatively insensitive to a frequency shift of the input pattern (from (u,v) to (u/a, v-bu/a), which results from the stereo transformation), since the factor $G (u + u_o, v + v_o)$ will usually be small. For this reason, one expects that tokens that favor phase filters are better behaved than those that emphasize the magnitude response.

To summarize: tokens that consist of a normalized combination of Gabor filters will be robust with respect to the stereo transformation, provided that:

(i) The filters have center frequencies along the v axis , or

(ii) The x component of the center frequency, u, satisfies

$$u \leq 1.25\ W \qquad (8)$$

where W is the spacing between the filters (in which case the average error will be "small").

2.2. Selectivity of Gabor Tokens.

Suppose we measure the distance between tokens using the L_1 norm. The selectivity of a token may be measured by the probability:

$$Pr\left[T_L(p_l) - T_R(p_r) < T_L(p_l) - T_R(q_r) \quad , \text{for all } q_r \neq p_r \right]$$

where p_l and p_r are corresponding points in the left and right images, and q_r is any other point in the right image, along the same epipolar line. Now, if the value of a physical observation has a certain probability of being incorrect, this probability decreases if one defines a new measurement as the average of a certain number n of independent observations, simply because the variance of the average is n times smaller than the variance of a single measurement, and the probability of failure is proportional to this variance. A precise quantification of this effect in our case is difficult to do, without the introduction of unrealistic assumptions about the nature of the probability distributions involved. It is clear, however, that increasing the number of independent filters that constitute a token, will increase its selectivity (see Kass, 1983). The price one pays is, of course, computational effort, but since the images may be passed through all the filters at the same time (given the hardware), this needs not affect the (parallel) speed of the computation.

2.3. Density.

Gabor tokens are "area based", and thus, in principle, they satisfy criterion (i). Filters with small values of σ, however, will have large frequency domain support, which means, first, that there are fewer independent filters available (the maximum number is given by the sampling theorem), so that the selectivity of the tokens will decrease, and also, that each filter may be "contaminated" by large u frequencies, so that the robustness of the token may also be affected. On the other hand, filters with large values of σ may misplace the depth discontinuities, and will have poor disparity resolution, particularly for curved surfaces.

One way out of this dilemma is to design a "coarse to fine" matching strategy:

Large tokens (i.e., tokens built with filters with large σ) are matched first, and the disparity computed with them is then used to constrain the valid disparity values of the smaller tokens, which are used to improve localization. The mechanism for this constraint propagation is discussed in the next section.

3. A Simple Model for Stereo Vision.

In this section we describe the construction of a stereo algorithm that uses Gabor tokens integrated in a coarse-to-fine matching strategy. The algorithm is intentionally simple, since the point we want to make here is that the use of these tokens makes both the correspondence and the surface reconstruction problems

trivial.

The complete system is schematized in figure 3:

---

figure 3 around here

The original pair of images R,L, is first passed through a bank of Gabor filters with large scale parameter; from the output of these filters, a set of magnitude and phase responses are computed, using equation (2). Let m_k , p_k denote the responses of the k^{th} filter. Next, the magnitude responses are normalized (dividing each one by their sum over all k), to eliminate the effect of the multiplicative constant in equation (5) (note that it is not necessary to normalize the phase responses). The matching procedure consists on the following steps:

1: for each point (x_o, y_o) do:

{

2: for each matching candidate in the same epipolar line (x, y_o) do:

{

3: for each filter k compute the distances:

$$dm_k(x) = |m_k(x_o, y_o) - m_k(x, y_o)| \ ;$$

$$dp_k(x) = \min(|d_k(x_o, y_o) - d_k(x, y_o)|, \ 2\pi - |d_k(x_o, y_o) - d_k(x, y_o)|) \ ;$$

compute :

$$dm(x) = \Sigma_k \, dm_k(x) \ ; \ dp(x) = \Sigma_k \, dp_k(x) \ .$$

}

4: Normalize dm and dp :

$$\overline{dm}\,(x) = (dm(x) - \inf_y dm(y)) \,/\, (\sup_y (dm(y) - \inf_y dm(y))$$

$$\overline{dp}\,(x) = (dp(x) - \inf_y dp(y)) \,/\, (\sup_y (dp(y) - \inf_y dp(y))$$

for all x.

5: Compute the disparity :

$$disp(x_o, y_0) = \arg \inf_x \{ \overline{dm}\,(x) + \overline{dp}\,(x) \}$$

}

This means that one chooses as a corresponding point, the one that minimizes (along an epipolar line) the normalized L_1 distance between the output of a set of Gabor filters acting on the left and right images. The normalization is necessary because the magnitude and phase distances are in different units, and thus, they cannot be added directly (slightly better results are obtained if the distances dm_k , dp_k are normalized separately for each k, so that the energy in each filter does not act as a weighting factor).

The disparity map thus obtained may have some deficiencies: if the scale parameter σ of the filter is large, the disparity resolution will be poor, particularly for curved surfaces; also, the depth discontinuities may be poorly localized, and there may be isolated pixels (or groups of pixels) which are assigned the wrong disparity. In order to refine these results, it may be necessary to repeat the matching procedure using filters with smaller σ. However, since these filters will be less robust and

selective, it is convenient to constrain the search for matching candidates (steps 2 and 3). This can be done by generating, using the coarse disparity map, a set of valid intervals where the true disparity, associated with each point, may lie.

These intervals may be obtained directly from the peaks of the local disparity histogram (of the coarse disparity map), taken over the support of the corresponding filters: one may simply select the intervals as the "domains" of the largest peaks, provided they are above a given threshold (we define the "domain" of a peak - a local maximum - as the interval spanned by the two adjacent local minima. In all cases, a peak was considered "significant" if the area under the curve in its domain was above 5 % of the total area under the histogram).

This scheme offers several advantages:

(i) Isolated small patches with spurious disparity values are automatically eliminated.

(ii) In the vecinity of depth discontinuities, the histogram becomes strongly multimodal (see Spoerry and Ullman, 1987); this implies that multiple intervals, associated with the disparities of the adjacent continuous regions, will be generated, so that finer filters may improve on the localization of their boundaries.

(iii) The location of the largest peak may be used to construct a high quality "Histogram-filtered" disparity map at each level.

(iv) The procedure is distributed, so that it can be efficiently implemented in parallel hardware.

The whole procedure may be iterated several times, obtaining, at each step, a disparity image that is a refinement of the preceding one. We have implemented a 3 step scheme, using values for σ of 3.8, 1.8 and 0.8 pixels. The experimental results are presented in section 5.

4. Feedback.

For a given stereo pair, some Gabor filters may be more robust and selective than others. This difference of performances may depend, among other things, on the frequency spectra of the images and of the noise, on the average size of locally planar regions, etc. Since the complete array of filters gives a very good response, one may use this total response to qualify the performance of each individual filter. These performance indices may then be fed back to the matching stage, so that only the best filters are used.

This procedure may also be used to compute statistics of the performance of each filter over several images, to see if - as one hopes - some filters are consistently better than others, so that an optimal set may be defined (at least for a class of images).

We may define several performance measures, for example:

(i) The average, over the whole image, of the distance found by each filter (i.e. dm_k or dp_k) at the point selected as "corresponding" by the whole set of filetrs, divided by the average distance found by the same filter over the whole epipolar line.

(ii) The total number of times that the point selected as "corresponding" by the whole set would also have been selected by the filter in question (i.e., the total number of times that the global minimum of dm_k (or dp_k) coincides with the global minimum of the sum of normalized distances).

(iii) The normalized sum of (i) and (ii).

We have measured experimentally the performance of a whole array of filters, using the three measures described above. The results, presentcd in the next section, are consistent with the analysis outlined in section 2.

5. Experimental Results.

We have implemetnted the system described in section 3, and applied it to a pair of images of a real scene. The results are presented in figures 4 - 11 :

Figure 4 shows the original stereo pair: a scene consisting of two painted cans ; figures 5, 6 and 7 show the output at the first, second and third matching stages, with sets of filters with scale

parameters σ = 3.8, 1.8 and 0.8, respectively (blank pixels mean that the disparity was outside the range [0,100]). The center frequencies are given in table 1 (in all cases, the spatial kernels were truncated for $|x|$ or $|y| > 3\sigma$, and we assigned to the magnitude distances dm_k, a relative weight of 0.8 with respect to the phase distances) .

Table 1 and figs. 4-11 around here.

Figure 8 shows the output of the "histogram filtering" at stage three. As one can see, the results are very good, except at the bottom of the image. This portion corresponds to the table where the TV camera lied. It is, therefore, out of focus, and even human observers would have trouble getting a good stereo response in this region. Figure 9 shows the limits for the valid disparity computed from the output of matching stage 1, and figure 10 shows the values of the performance index (iii) for the magnitude and phase responses of the complete set of filters at stage 2 (σ = 1.8).

Finally, figure 11 shows the Histogram-filtered disparity image, obtained directly from the original stereo pair by applying only the 7 filters that had the highest performance index at stage 2. These are phase filters with center frequencies at: (0,.2), (0,.4), (.2,±.4), (.2,±.2) and (.2,0). As one can see, even this one-stage simple matcher gives excellent results.

5. Discussion.

From the limited experiments we have performed so far, one can

make the following observations:

(i) Tokens constructed with the output of a set of magnitude and phase Gabor filters are very effective for stereo matching, to the extent that one can get very good results with trivial matching rules (i.e., take the minimal normalized distance).

(ii) Since these filters are area based, they produce dense disparity maps, so that the surface reconstruction step is greatly simplified.

(iii) Using a simple coarse to fine matching strategy, one can get very good localization of depth discontinuities.

(iv) The filters that give the best response, with respect to the matching task, have center frequencies that lie within an ellipse, centered at (0,0), in the spatial frequency domain. It extends vertically, up to ± 60 % of the Nyquist frequency, and horizontally, up to ± 40 % .

(v) Phase filters tend to give better responses than magnitude ones (the performance index ratio is ≈ 1.3 : 1).

The role that these tokens may play in the construction of practical, real-time stereo systems will depend on the development of appropriate parallel hardware. Given this hardware, the scheme that we outline here may have a high computational efficiency. At this point, its main interest lies in its plausibility as a model

for biological stereo matching.

A conclusion that should NOT be drawn from these results, is that more powerful methods for solving the correspondence and surface reconstruction problems (e.g., enforcement of the uniqueness constraint; incorporation of prior knowledge about the solution, etc.) are superfluous. The point that we wish to make is just that the use of high-performance tokens may greatly simplify the task of these more sophisticated mechanisms, that can be made to operate preferently in problematic areas of an image, after a coarse estimate of disparity is obtained in a first, "fast and dirty" stage.

Work is still needed to refine these results. In particular, we plan to gather more experimental data (process more images), and refine the performance analysis. Also, we are investigating the incorporation of other processes (such as color, motion and texture) into the stereo processing.

Acknowledgements : I wish to thank Ricardo Berlanga for many useful discussions. The images used for this work were generated with the help of the Centro de Investigaciones en Optica, Leon, Gto., Mexico.

Table 1. Center Frequencies for the 3 Matching Stages.

Stage 1		Stage 2		Stage 3	
u	v	u	v	u	v
0	.1	0	.2	0	.2
0	.2	0	.4	0	.5
0	.3	0	.6	.3	-.3
0	.4	.2	-.4	.3	0.
0	.5	.2	-.2	.3	.3
0	.6	.2	0.		
.1	-.4	.2	.2		
.1	-.2	.2	.4		
.1	0.	.4	-.4		
.1	.2	.4	-.2		
.1	.4	.4	0.		
.2	-.6	.4	.2		
.2	-.4	.4	.4		
.2	-.2				
.2	0.				
.2	.2				
.2	.4				
.2	.6				

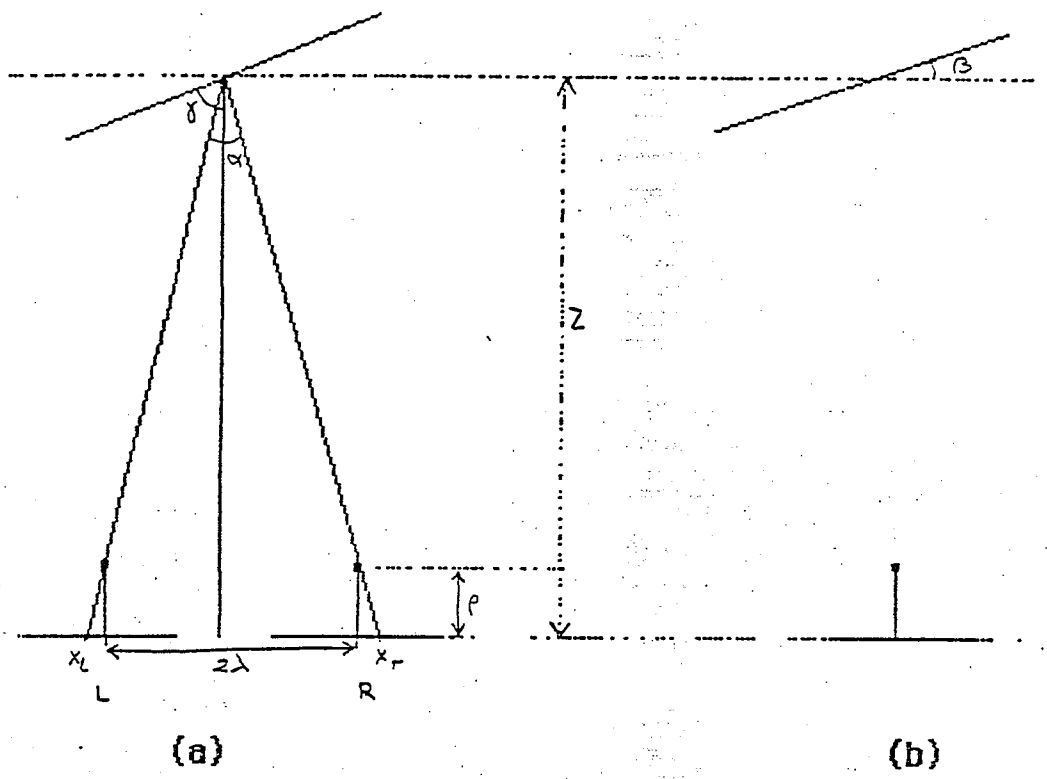

Figure 1. Geometry associated with the formation of a stereo pair of images of a plane. (a) Top view. (b) Side view.

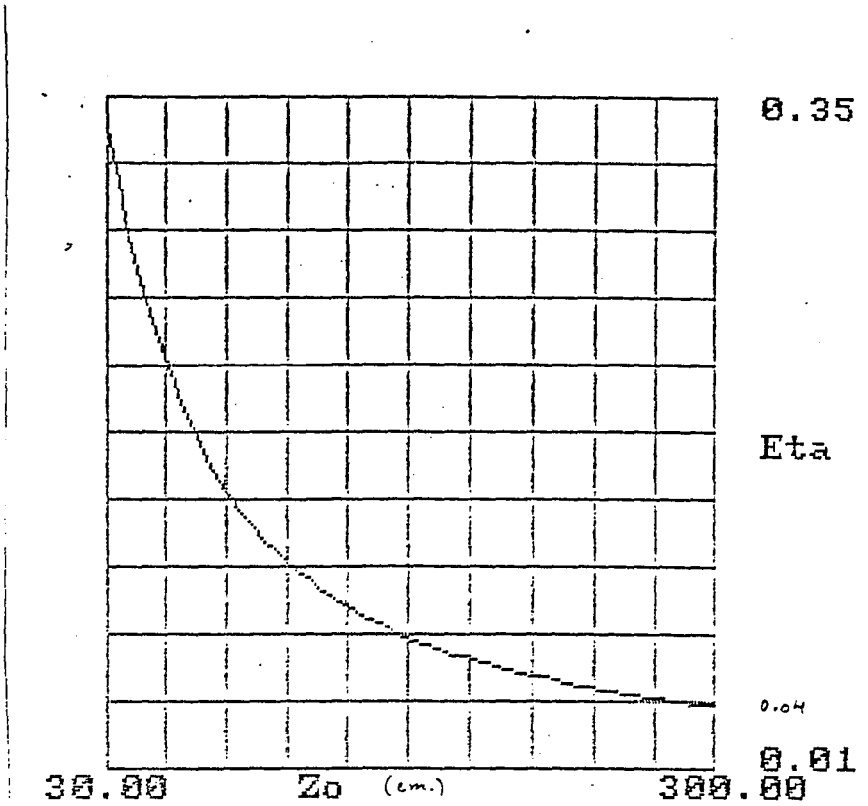

Figure 2. Average value of the error factor η vs. Z (see text).

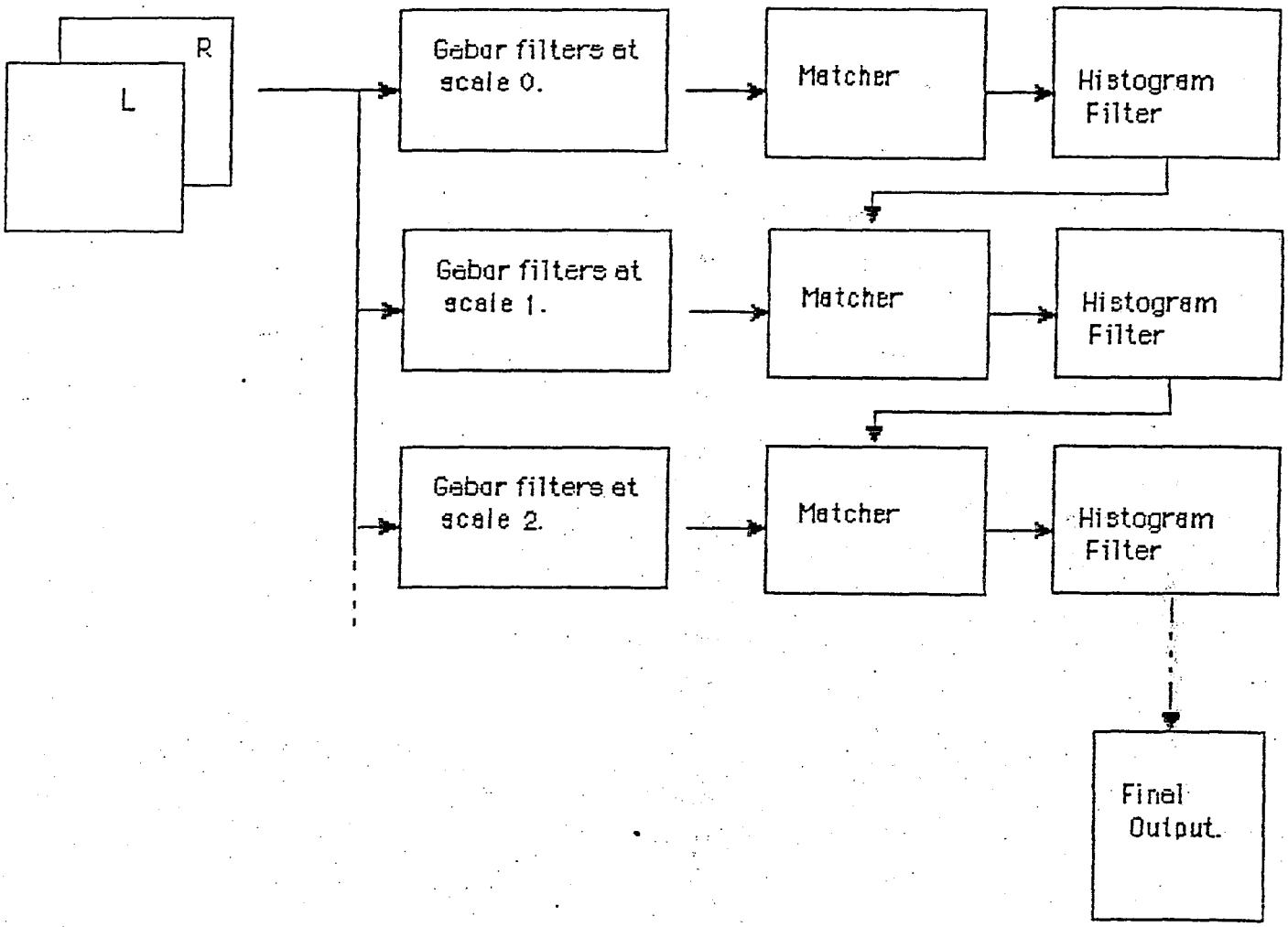

Figure 3. A simple model for stereo vision (see text).

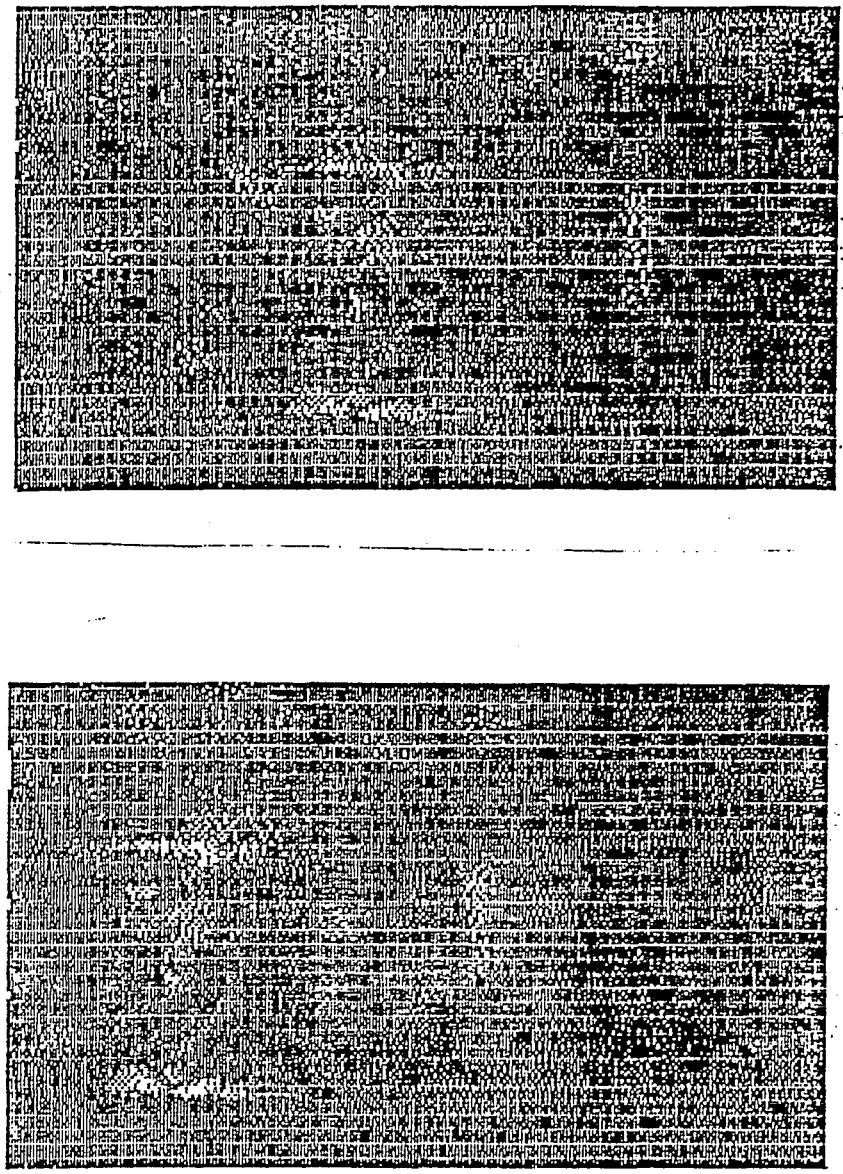

Figure 4. Stereo pair of a scene consisting on two painted cans. Top panel: left component; bottom panel: right component.

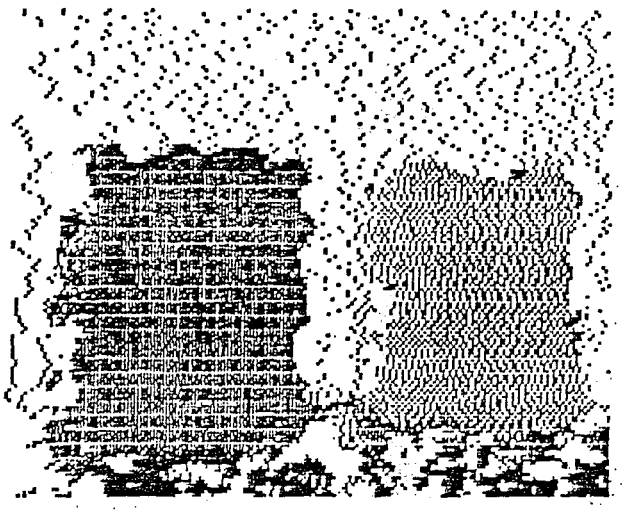

Figure 5. Disparity image (output of the matcher) at level 1 (σ = 3.8). Disparity values are coded by grey level.

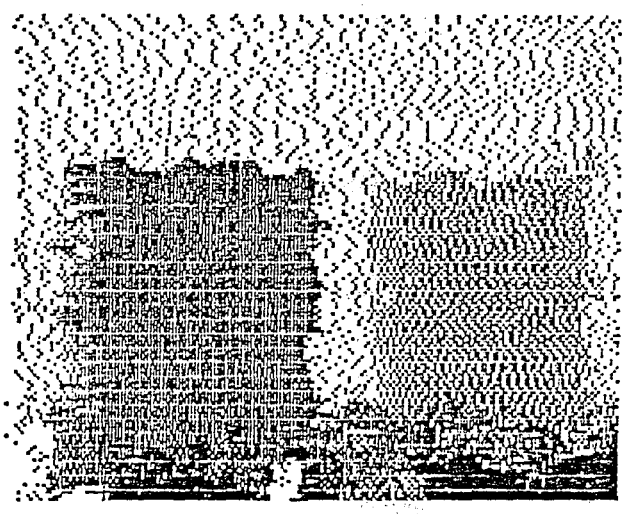

Figure 6. Disparity image (output of the matcher) at level 2 (σ = 1.8). Disparity values are coded by grey level.

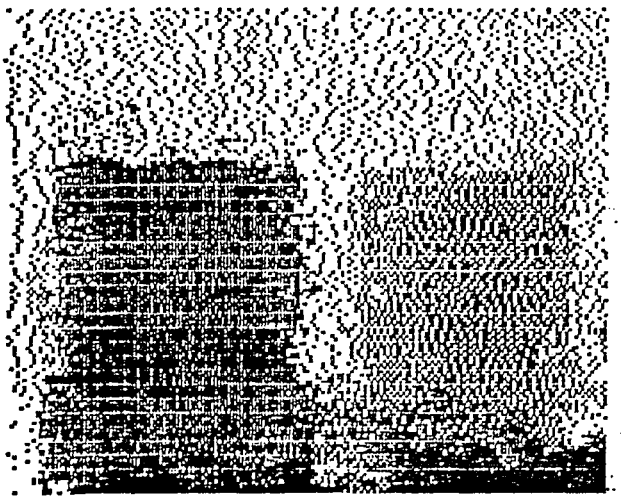

Figure 7. Disparity image (output of the matcher) at level 3 (σ = 0.8). Disparity values are coded by grey level.

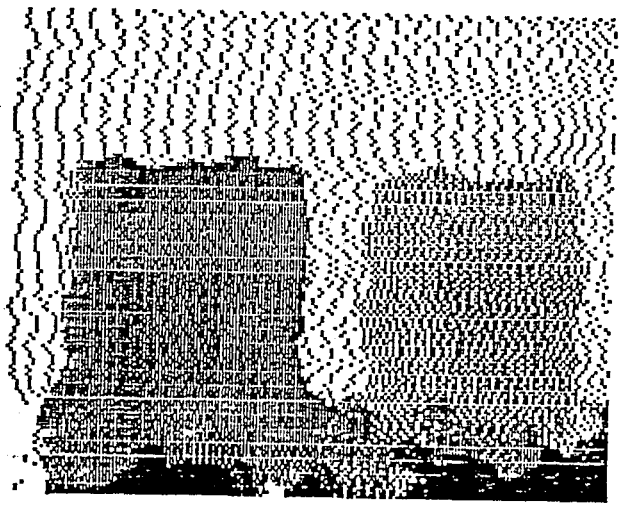

Figure 8. Disparity image obtained at the output of the histogram filter at level 3 (σ = 1.8). Disparity values are coded by grey level.

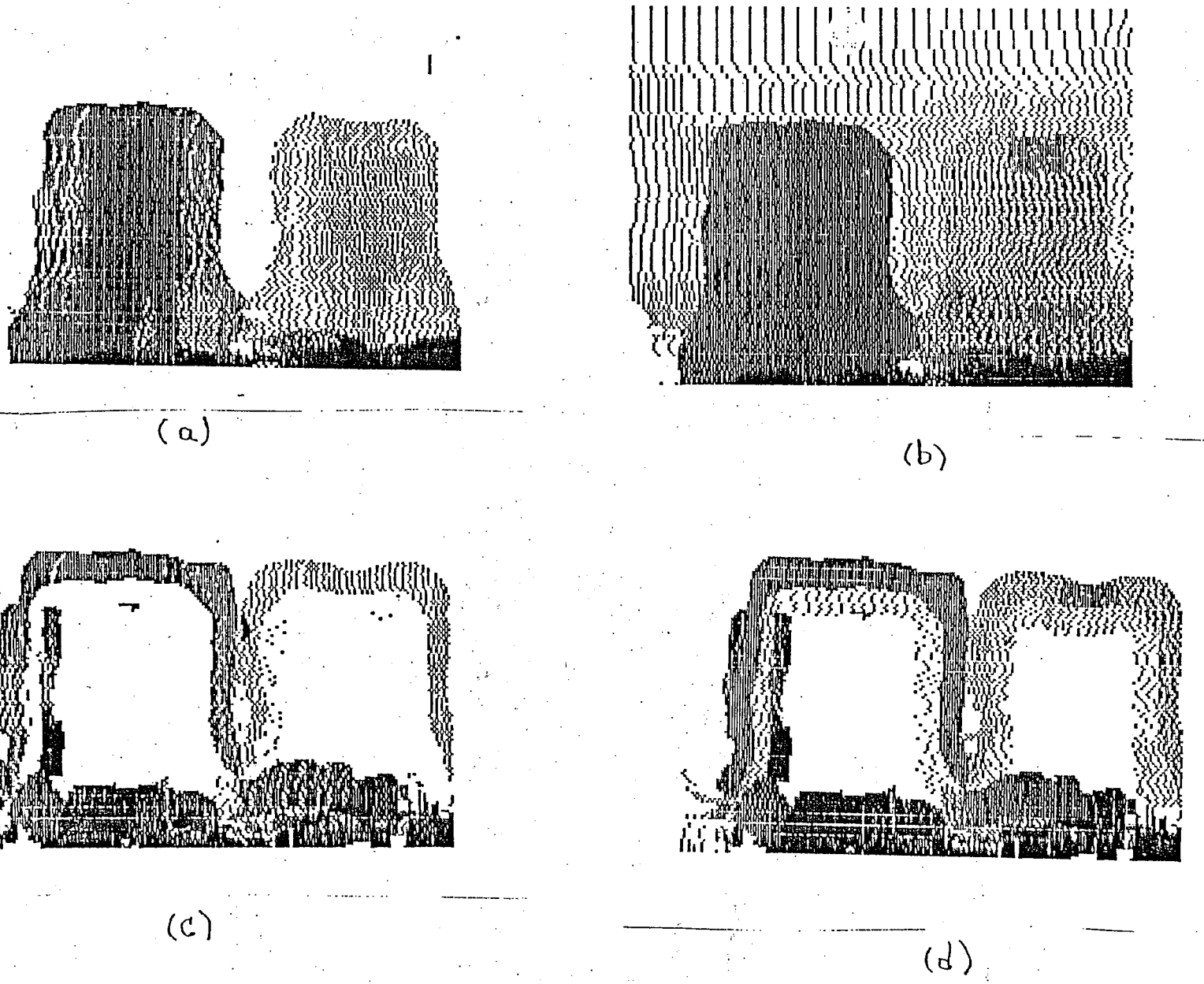

Figure 9. Limits for the valid disparity computed from the output of the matcher at level 0. (a) Lower limit from the largest peak of the local histogram. (b) Upper limit. (c) Lower limit from the second largest peak. (d) Upper limit.

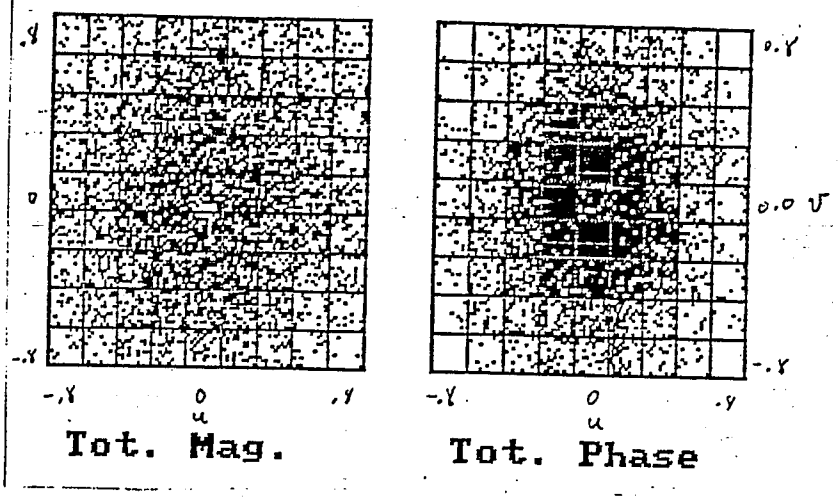

Figure 10. Values (coded by grey level) of the performance index for the complete set of filters with scale parameter σ = 1.8.

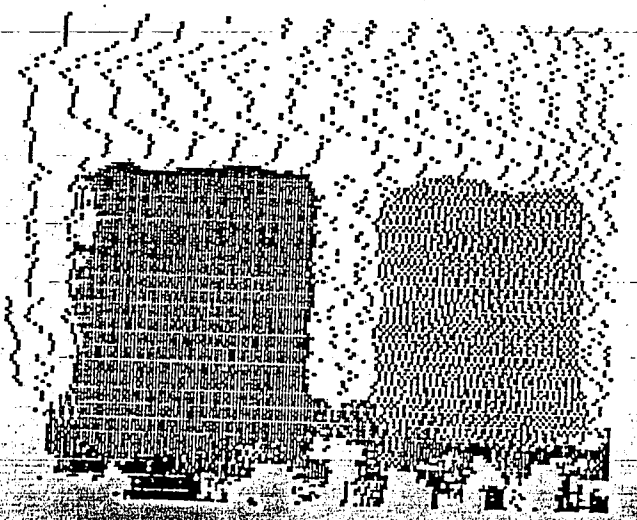

Figure 11. Disparity image obtained after Histogram-filtering the output of the matcher, using as level 1 the 7 phase filters with highest performance index, with scale parameter σ = 1.8.